PROCEEDINGS OF SCIENCE

Beauty to charmonium decays at LHCb

Peilian Li[1,*]

Heidelberg University,
Im Neuenheimer Feld 226, Heidelberg, Germany

E-mail: peilian.li@cern.ch

The latest results of beauty meson decays to final states with charmonium resonances from LHCb are presented. This includes measurements of time-dependent CP violation parameters in $B_s^0 \to J/\psi K^+K^-$ and $B_s^0 \to J/\psi \pi^+\pi^-$ decay modes. Combined with the measurements from other decay modes, the latest world average of ϕ_s value is $\phi_s = (-0.051 \pm 0.023)$ rad, dominated by the LHCb measurements.

40th International Conference on High Energy physics - ICHEP2020
July 28 - August 6, 2020
Prague, Czech Republic (virtual meeting)

[1]On behalf of the LHCb Collaboration
[*]Speaker

PoS(ICHEP2020)390

1. CP violation in the $B_s^0 - \bar{B}_s^0$ system

The existence of new phenomena beyond those predicted by the Standard Model (SM), as known as New Physics (NP), could introduce sizeable effects on CP-violating observables. In the SM, CP violation originates from an irreducible complex phase in the Cabibbo-Kobayashi-Maskawa (CKM) matrix that describes the mixing of the mass and weak interaction eigenstates of the quarks. In the $B_s^0 - \bar{B}_s^0$ system, CP violation can originate from the interference of the decay amplitude of B_s^0 to its CP eigenstates, and that of the adjoint decay preceded by $B_s^0 - \bar{B}_s^0$ oscillation. The corresponding CP violating phase, ϕ_s, can be expressed in terms of CKM matrix elements as $-2\arg[-V_{ts}V_{tb}^*/V_{cs}V_{cb}^*]$ by ignoring penguin contributions. Assuming unitarity of the CKM matrix, global fits to experimental data give a precise prediction of $\phi_s = (-0.0369^{+0.0010}_{-0.0007})$ rad according to the CKMfitter group [1] and of $\phi_s = (-0.0370 \pm 0.0010)$ rad according to the UTfit collaboration [2]. Such precise prediction of ϕ_s in the SM makes its measurement particularly interesting because any New Physics contributing to the $B_s^0 - \bar{B}_s^0$ mixing diagrams could potentially modify the phase [3]. The value of ϕ_s measured to be significantly different from the SM would be a clear evidence for physics beyond the SM.

2. Measurement of ϕ_s in $B_s^0 \to J/\psi h^+ h^-$ at LHCb

Two recent measurements of the phase ϕ_s through $B_s^0 \to J/\psi h^+ h^-$[1] ($h^+h^- = K^+K^-$ [4], or $\pi^+\pi^-$ [5]) decays at the LHCb experiment are presented. The single measurement in $B_s^0 \to J/\psi K^+K^-$ mode provides the most precise result in the world. As the analysis strategies are very similar, the baseline strategy adopted by both is covered and relevant differences between the two are explicitly stated.

Both analyses use proton-proton collision data collected with the LHCb detector in 2015 and 2016, corresponding to a total integrated luminosity of 1.9 fb^{-1}. A B_s^0 meson flies approximately 1 cm before decaying inside the vertex locator (VELO) of the LHCb detector [6], after being produced in a proton-proton collision inside the VELO (so-called primary vertex). The excellent resolution of the VELO detector, which is around 45 fs (42 fs) for the $B_s^0 \to J/\psi K^+K^-$ ($B_s^0 \to J/\psi\pi^+\pi^-$) mode, allows to resolve the oscillation in $B_s^0 - \bar{B}_s^0$ system. The decay products of a B_s^0 meson, $J/\psi K^+K^-$ or $J/\psi\pi^+\pi^-$ where J/ψ decays to $\mu^+\mu^-$ pair, fly from the decay point of B_s^0 (secondary vertex) through the detector, traversing the magnet to tracking stations, Cherenkov detector, calorimeter system and muon stations. The tracks of charged particles are reconstructed with the hits in the tracking stations, and extrapolated further for particle identification.

CP-violating parameters ϕ_s and $|\lambda|$ are measured in both $B_s^0 \to J/\psi K^+K^-$ and $B_s^0 \to J/\psi\pi^+\pi^-$ channels. Angular momentum conservation in the decay implies that the final state is an admixture of CP-even and CP-odd components, with orbital angular momentum of 0 or 2, and 1, respectively. This allows measuring lifetime parameters of the B_s^0 meson: the decay-width difference between the heavy and light B_s^0 meson eigenstates, $\Delta\Gamma_s = \Gamma_L - \Gamma_H$, and the average decay-width of the states, $\Gamma_s = \frac{\Gamma_L+\Gamma_H}{2}$. However, since $B_s^0 \to J/\psi\pi^+\pi^-$ final state is almost entirely CP-odd [7], $B_s^0 \to J/\psi\pi^+\pi^-$ channel allows the determination of the decay width of the heavy B_s^0 mass

[1]The inclusion of charge-conjugate processes is implied throughout this manuscript, unless otherwise noted.

eigenstate, Γ_H. The possible presence of a CP-even component (with fraction below 2.3% at 95% confidence level) is taken into account when determining ϕ_s.

In order to disentangle the CP-even and CP-odd components, a decay-time-dependent angular analysis is performed, where the angular observables $\cos\theta_{\rm h}$, $\cos\theta_\mu$ and ϕ_h are defined in the helicity basis as described in Ref. [8]. The physics parameters are extracted from a simultaneous maximum likelihood fit to the decay-time and three angles distributions. The parametrization of these distributions is given as a function of the decay time and angles, as shown below:

$$\frac{d^4\Gamma}{dtd\Omega} \propto \sum_{k=1}^{10} \epsilon(t,\Omega) f_k(\Omega) h_{k,q}(t) \otimes G(t|\sigma_t), \tag{1}$$

where, Ω represents the three angles (θ_h, θ_μ and ϕ_h) of the helicity basis and $q = \pm 1$ corresponds to the initial flavour of the $B_s^0/\bar{B}_s^0$ meson, $\epsilon(t,\Omega)$ is efficiency as a function of decay-time and angular observables, $f_k(\Omega)$ are angular functions, $G(t|\sigma_t)$ is experimental decay-time resolution and the decay-time-dependent functions $h_{k,q}(t)$ for the decay of B_s^0 meson are given as

$$h_{k,q=\pm1}(t) = \frac{3}{4\pi} e^{-\Gamma t} \{a_k \cosh\frac{\Delta\Gamma t}{2} + b_k \sinh\frac{\Delta\Gamma t}{2} \pm c_k \cos(\Delta m t) \pm d_k \sin(\Delta m t)\}. \tag{2}$$

To perform the time-dependent fit, several experimental inputs such as efficiency, decay-time resolution of the detector and the knowledge of the flavour of the B_s^0 meson at production, are required. In the case of $B_s^0 \to J/\psi\pi^+\pi^-$ decay, the invariant mass of two pions is also an observable in the fit (5D fit), where the efficiency as a function of the invariant mass is studied separately. While for $B_s^0 \to J/\psi K^+K^-$ decay, the kaon pair predominantly originates from the decay of a $\phi(1020)$ resonance. Therefore, the invariant mass of two kaons is divided into 6 bins in ϕ mass region to account for the different contribution of non-ϕ component in each bin. The details are given in the following.

2.1 Selection and mass fit

The time-dependent angular fit is performed on background-subtracted data. For both channels, a Boosted Decision Tree [9], BDT, is used to select signal and reject background candidates. The BDTs are trained with simulated signal events as signal proxy and data sidebands as background proxy. In the $B_s^0 \to J/\psi K^+K^-$ channel, significant peaking background contribution from $\Lambda_b \to J/\psi p K^+$ due to mis-identification of proton as kaon is subtracted by injected negatively weighted simulated sample of $\Lambda_b \to J/\psi p K^+$ decays with the total weight equal to the expected contribution of the Λ_b background. Other contributions coming from decays $B^0 \to J/\psi K^+K^-$ and $B^0 \to J/\psi K^{*0}(\to K^+\pi^-)$ are either vetoed using particle identification requirements or accounted for directly in the mass fit.

An sPlot [10] procedure is used to disentangle the combinatorial background events from the signal candidates by assigning a signal weight to each event based on the probability density function (PDF) that is used to describe the invariant mass spectra. The invariant mass distributions of $J/\psi K^+K^-$ and $J/\psi\pi^+\pi^-$ are shown in Fig. 1 together with the analytical shapes that are used to extract the signal weights.

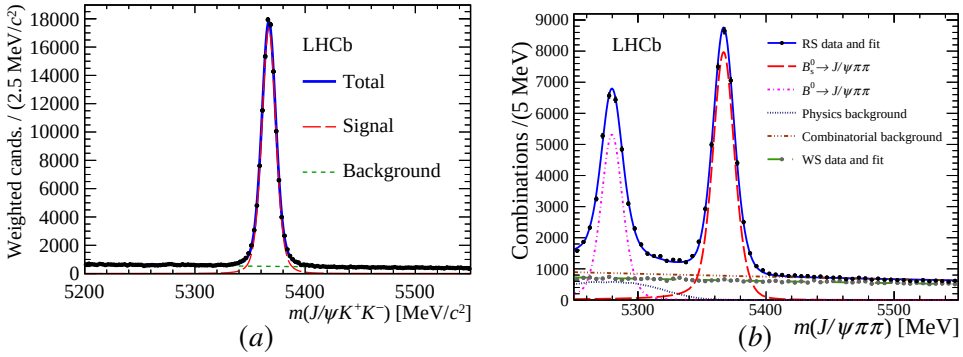

Figure 1: Distribution of the invariant mass of selected (a) $B_s^0 \to J/\psi K^+K^-$ and (b) $B_s^0 \to J/\psi\pi^+\pi^-$ decays. The color-coding of PDFs are explained on the plots.

2.2 Decay time resolution

The decay-time resolution of the detector directly affects the precision of the measured CP-violating parameters. Thus, the knowledge of the decay-time resolution calibration is pivotal. The prompt data samples that consist of $J/\psi \to \mu^+\mu^-$ candidates and h^+h^- tracks that originate from the primary vertex and therefore have zero lifetime, are used to perform the decay-time resolution calibration. The averaged effective single-Gaussian resolutions are estimated to be $\sigma_{\text{eff}} = 45.5$ fs for $B_s^0 \to J/\psi K^+K^-$ and $\sigma_{\text{eff}} = 41.5$ fs for $B_s^0 \to J/\psi\pi^+\pi^-$, respectively.

2.3 Reconstruction and selection efficiency

The geometry of the detector together with the selection requirements cause non-uniform efficiency as a function of the observables (decay-time and helicity angles). For both decay modes, efficiency as a function of helicity angles is evaluated with simulated signal events that have been weighted to match the kinematics and physics of the signal modes in data.

The non-uniform shape of the efficiency as a function of decay-time is caused by biasing selection introduced already in the trigger stage and is described with cubic splines. Since the simulation is not completely reliable in modeling of trigger response, a data-driven method is used in both decay channels. The kinematically similar mode $B^0 \to J/\psi(\to \mu^+\mu^-)K^*(892)^0(\to K^+\pi^-)$ is taken as a control sample, which has a well-known lifetime of $\tau_{B^0} = 1.520 \pm 0.004$ ps [11]. The B_s^0 efficiency is determined via a simultaneous fit to background-subtracted data and simulated samples through the relation $\epsilon^{B_s^0}_{\text{data}}(t) = \epsilon^{B^0}_{\text{data}}(t) \times \epsilon^{B_s^0}_{\text{sim}}(t)/\epsilon^{B^0}_{\text{sim}}(t)$, where $\epsilon^{B^0}_{\text{data}}(t)$ is the efficiency of the control mode and $\epsilon^{B_s^0}_{\text{sim}}(t)/\epsilon^{B^0}_{\text{sim}}(t)$ is the ratio of efficiencies of simulated signal and reference decays after full reconstruction and selection. Residual differences between either signal and control mode or data and simulation are corrected by applying weight to match the kinematics variables and invariant mass distributions of the signal data candidates.

2.4 Results

Taking into account the decay-time resolution and efficiencies described above, a time-dependent maximum likelihood fit is performed to extract the parameters of interest. The corresponding background-subtracted data distributions with fit projections for the $B_s^0 \to J/\psi K^+K^-$

Table 1: Measured physics parameters obtained with $B_s^0 \to J/\psi K^+K^-$ and $B_s^0 \to J/\psi \pi^+\pi^-$ decay modes at LHCb, as well as the ones combining all the measurements available at LHCb. If two uncertainties are given, the first is statistical and the second systematic; otherwise, it is a combination of both statistical and systematic uncertainties.

Decay mode	$B_s^0 \to J/\psi K^+K^-$	$B_s^0 \to J/\psi \pi^+\pi^-$	LHCb combination
$\phi_s\ [rad]$	$-0.080 \pm 0.041 \pm 0.006$	$-0.057 \pm 0.060 \pm 0.011$	-0.041 ± 0.025
$\lvert\lambda\rvert$	$1.006 \pm 0.016 \pm 0.006$	$1.01^{+0.08}_{-0.06} \pm 0.03$	0.993 ± 0.010
$\Gamma_{s/H} - \Gamma_{B^0}\ [ps^{-1}]$	$-0.0041 \pm 0.0024 \pm 0.0015$	$-0.050 \pm 0.004 \pm 0.004$	$\Gamma_s = 0.6562 \pm 0.0021$
$\Delta\Gamma_s\ [ps^{-1}]$	$0.0772 \pm 0.0077 \pm 0.0026$	-	0.0816 ± 0.0048

and $B_s^0 \to J/\psi \pi^+\pi^-$ channels are shown in the upper and bottom row of Fig. 2, respectively. The physics parameters obtained in two analyses are summarized in Table 1. The results are in good agreement with each other, as well as with the previous LHCb measurement.

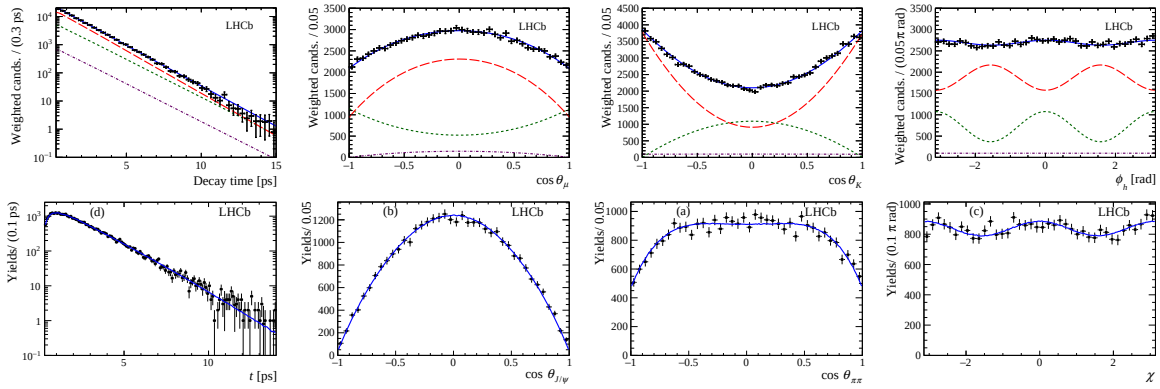

Figure 2: Distribution of the invariant mass of selected (upper row) $B_s^0 \to J/\psi K^+K^-$ and (bottom row) $B_s^0 \to J/\psi \pi^+\pi^-$ decays. The black dots are data, the blue curves are the fit projections of total PDFs, the red long-dashed, green dashed and purple dotted curves in the upper plots are the projections of CP-even, CP-odd and S-wave components, respectively.

Using a minimum χ^2 fit, the presented results are combined with other available LHCb measurements [12], taking into account all statistical correlations, all systematic errors and their correlations, and correlations between different run periods. As shown in the last column of Table 1, the combined values of these parameters are the most precise to date. Figure 3(a) shows the 68% confidence level regions in the ϕ_s versus $\Delta\Gamma_s$ plane for the considered analyses and the LHCb combination. The combined value of ϕ_s is consistent with global fits to data. The parameter $|\lambda|$ agrees with the hypothesis of no CP violation in the decay. The values of Γ_s and $\Delta\Gamma_s$ are consistent with expectations from HQE models. Figure 3(b) shows the combined results including the measurements from other experiments.

3. Summary

In summary, the flavour-tagged decay-time-dependent angular analyses of $B_s^0 \to J/\psi K^+K^-$ and $B_s^0 \to J/\psi \pi^+\pi^-$ decays are presented, in which the measurement of ϕ_s in single channel

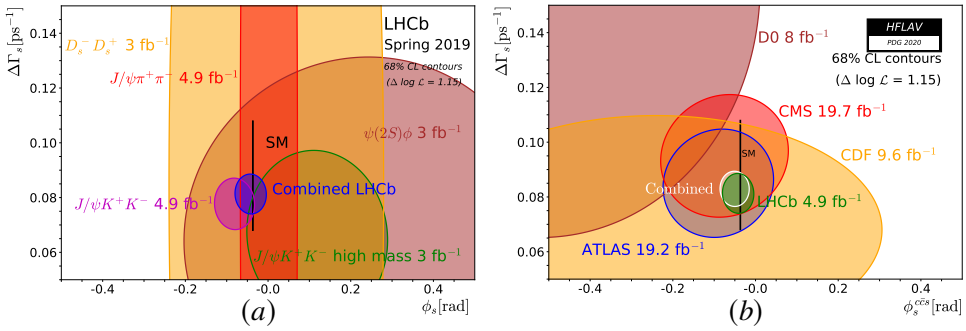

Figure 3: (a) Regions of 68% confidence level in the $\phi_s - \Delta\Gamma_s$ plane for the individual LHCb measurements and a combined contour (in blue). (b) Regions of 68% confidence level in the $\phi_s - \Delta\Gamma_s$ plane for the combined measurements from different experiments.

$B_s^0 \to J/\psi K^+K^-$ is the most precise to date. The latest world-average value of $\phi_s = (-0.051 \pm 0.023)$ rad [13] is dominated by the measurements from LHCb. However, the results are all statistically limited. It will be further improved with run 3 and 4.

References

[1] CKMfitter group, J. Charles *et al.*, Phys. Rev. D **91**, 073007 (2015), arXiv:1501.05013, updated results and plots available at http://ckmfitter.in2p3.fr/.

[2] UTfit Collaboration, M. Bona *et al.*, JHEP **10**, 081 (2006), arXiv:hep-ph/0606167, updated results and plots available at http://www.utfit.org/.

[3] A.J.Buras, PoSEPS-HEP2009, 024 (2009), arXiv:0910.1032; C.-W. Chiang *et al.*, JHEP **04**, 031 (2010), arXiv:0910.2929.

[4] LHCb Collaboration, R. Aaij *et al.*, Eur. Phys. J. C **79**, 706 (2019), arXiv:1906.08356.

[5] LHCb Collaboration, R. Aaij *et al.*, Phys. Lett. B **797**, 134789 (2019), arXiv:1903.05530.

[6] LHCb Collaboration, R. Aaij *et al.*, Int. J. Mod. Phys. A **30**, 1530022 (2015), arXiv:1412.6352.

[7] LHCb collaboration, R. Aaij *et al.*, Phys. Rev. D **89** 092006 (2014), arXiv:1402.6248.

[8] LHCb Collaboration, R. Aaij *et al.*, Phys. Rev. D **87**, 112010 (2013), arXiv:1304.2600.

[9] L. Breiman, J.H. Friedman, R.A. Olshen, C.J. Stone (Wadsworth international group), Classification and Regression Trees, Belmont, (1984).

[10] M. Pivk, F.R. Le Diberder, Nucl. Instrum. Methods A **555**, 356 (2005), arXiv:physics/0402083.

[11] Particle Data Group, M. Tanabashi *et al.*, Phys. Rev. D **98**, 030001 (2018).

[12] LHCb Collaboration, R. Aaij *et al.*, Phys. Rev. Lett. **114**, 041801 (2015); Phys. Lett. B **736**, 186 (2014); Phys. Lett. B **762**, 253 (2016); Phys. Rev. Lett. **113**, 211801 (2014); JHEP **08**, 037 (2017).

[13] https://hflav-eos.web.cern.ch/hflav-eos/osc/PDG_2020/